A classical-map simulation of two-dimensional electron fluid: an extension of classical-map hypernetted-chain theory beyond the hypernetted-chain approximation

2009 J. Phys.: Condens. Matter 21 045502

(http://iopscience.iop.org/0953-8984/21/4/045502)

IOP Publishing Journal of Physics: Condensed Matter
J. Phys.: Condens. Matter **21** (2009) 045502 (7pp) doi:10.1088/0953-8984/21/4/045502

A classical-map simulation of two-dimensional electron fluid: an extension of classical-map hypernetted-chain theory beyond the hypernetted-chain approximation

Chieko Totsuji, Takashi Miyake, Kenta Nakanishi, Kenji Tsuruta and Hiroo Totsuji

Graduate School of Natural Science and Technology and Faculty of Engineering, Okayama University, Tsushimanaka 3-1-1, Okayama 700-8530, Japan

E-mail: totsuji@elec.okayama-u.ac.jp

Received 8 October 2008
Published 15 December 2008
Online at stacks.iop.org/JPhysCM/21/045502

Abstract
A method for numerically simulating quantum systems is proposed and applied to the two-dimensional electron fluid at $T = 0$. This method maps quantum systems onto classical ones in the spirit of the classical-map hypernetted-chain theory and performs simulations on the latter. The results of the simulations are free from the assumption of the hypernetted-chain approximation and the neglect of the bridge diagrams. A merit of this method is the applicability to systems with geometrical complexity and finite sizes including the cases at finite temperatures. Monte Carlo and molecular dynamics simulations are performed corresponding to two previous proposals for the 'quantum' temperature and an improvement in the description of the diffraction effect. It is shown that one of these two proposals with the improved diffraction effect gives significantly better agreement with quantum Monte Carlo results reported previously for the range of $5 \leqslant r_s \leqslant 40$. These results may serve as the basis for the application of this method to finite non-periodic systems like quantum dots and systems at finite temperatures.

1. Introduction

Properties of electron systems in three or two dimensions are of basic importance in designing various materials as electronic devices. In spite of a long history of their investigations, we still lack simple and, at the same time, accurate methods applicable to these quantum systems. With the development of mesoscopic manufacturing especially in two dimensions, there seems to exist an enhanced requirement for a theoretical framework to handle two-dimensional electron systems of mesoscopic scale. We here analyze the validity of a method which is based on a mapping to classical systems and easily applicable to finite systems and systems at finite temperatures.

Dharma-wardana and Perrot developed the classical-map hypernetted-chain (CHNC) theory [1] so as to reproduce the results of first-principle quantum simulations for uniform interacting electron fluid by mapping a quantum system to a classical system. This mapping includes the introduction of a 'quantum temperature', modification of the Coulomb interaction, and an additional potential between electrons with the same spins. This theory has been applied to infinite electron fluids in two and three dimensions and a variety of physical properties have been analyzed at zero and also at finite temperatures with arbitrary spin polarization [1–6].

The CHNC analyses by Dharma-wardana and Perrot have been made on uniform unbounded systems through integral equations which are simplified due to the translational invariance. For systems without the latter invariance or those with complicated geometry, however, it is not straightforward to apply the integral equations. Typical examples may be quantum dots or multi-layered electron systems.

We propose a method of numerical simulation based on the mapping of the CHNC theory. This simulation automatically takes the contribution of the bridge diagrams into account. The latter is not included within the hypernetted-chain equations and needs an extra element which is well established only for uniform systems. This simulation can be easily applied to systems without translational invariance and systems at finite temperatures.

In order to apply our method of simulation to these systems, it is necessary to confirm the applicability to uniform systems at $T = 0$ for which the results of *ab initio* simulations are known. Our purpose is to confirm the applicability of our method to systems with translational invariance and establish a basis for applications to other cases. We compare two mapping functions for the temperature proposed previously and give an improvement in the treatment of the diffraction effect.

We here consider the two-dimensional electron fluids. The system has the surface number density n and the temperature T, and we denote the spin components by suffices or superscripts $\sigma = \pm$:

$$n = \sum_{\sigma} n_{\sigma}. \tag{1}$$

Our system is characterized by three parameters: the r_s parameter defined by

$$r_s = (\pi n)^{-1/2}, \tag{2}$$

the spin polarization ζ defined by

$$\zeta = \frac{n_+ - n_-}{n_+ + n_-} = \frac{n_+ - n_-}{n}, \tag{3}$$

and the temperature T. We use the atomic units and take $k_B = 1$ in most expressions.

2. Outline of classical-map hypernetted-chain theory

The CHNC theory is composed of three elements [1]: (a) the assignment of the temperature to include the effect of degeneracy, (b) the addition of a repulsive potential (the Pauli potential) between electrons with the same spin component to simulate the effect of Fermi statistics, and (c) the modification of the Coulomb potential to include the effect of diffraction.

2.1. Quantum temperature

A quantum system at temperature T is assumed to be mapped onto the classical fluid at the temperature T_{cf} given by

$$T_{cf} = (T_q^2 + T^2)^{1/2}. \tag{4}$$

Here T_q is the 'quantum temperature' which expresses the effect of degeneracy in terms of a contribution to the temperature of classical fluid. Values of T_q are given as a function of r_s to reproduce the quantum pair distribution function in the ground state obtained by quantum Monte

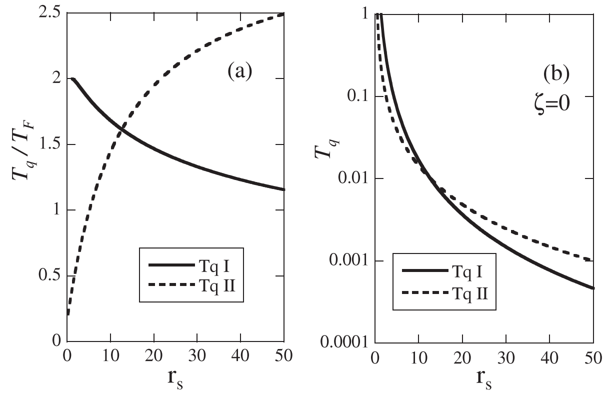

Figure 1. The comparison of mapping functions Tq I and Tq II, (a) T_q/T_F versus r_s, and (b) T_q versus r_s, for $\zeta = 0$ in atomic units.

Carlo simulations. For three-dimensional electron fluids, T_q is expressed as

$$T_q/T_F = 1/(a + b\, r_s^{1/2} + c\, r_s) \tag{5}$$

with $a = 1.594, b = -0.3160, c = 0.0240$ and $r_s = (4\pi n/3)^{-1/3}$, n being the electron density [1]. Here T_F is defined by

$$k_B T_F = \sum_{\sigma=\pm 1} \frac{n_\sigma}{n} E_F^\sigma \tag{6}$$

and E_F^σ is the Fermi energy of spin species σ.

For two-dimensional electron fluids, the relation (Tq I)

$$T_q/T_F = 2/[1 + 0.864\,13(r_s^{1/6} - 1)^2] \quad \text{(Tq I)} \tag{7}$$

has been proposed [2]. This is based on a comparison of the values of the correlation energy E_c of a fully polarized system with those obtained by Tanatar and Ceperley through the diffusion Monte Carlo (DMC) method [7]. Bulutay and Tanatar have proposed another expression (Tq II) for two-dimensional systems [4]:

$$T_q/T_F = \frac{1 + a\, r_s}{b + c\, r_s} \quad \text{(Tq II)} \tag{8}$$

with $a = 1.470\,342$, $b = 6.099\,404$, $c = 0.476\,465$ by fitting the correlation energy E_c of the unpolarized system to the result of Rapisarda and Senatore [8] obtained by DMC methods over the range $0.25 < r_s < 40$. As for the bridge diagrams, Tq I is determined by the analyses of the modified hypernetted-chain equation where their contribution is approximately taken into account. On the other hand, Tq II is determined within the hypernetted-chain approximation without their contribution.

These two expressions have significantly different dependence on r_s as shown in figure 1 while giving the same quantum temperature T_q/T_F at around $r_s = 12.5$. Though the detailed functional form of T_q does not directly affect the result, T_q is one of major ingredients of this method.

2.2. Pauli potential

The Pauli potential between electrons with the same spin species is determined so as to reproduce the exact correlation in the ideal Fermi gas within the hypernetted-chain approximation. In a classical fluid at the temperature $T_{\rm cf}$, the pair distribution function between particles of species σ and σ' is generally written as

$$g_{\sigma\sigma'}(r) = \exp[-\beta\,\phi_{\sigma\sigma'}(r)+h_{\sigma\sigma'}(r)-c_{\sigma\sigma'}(r)+B_{\sigma\sigma'}(r)], \quad (9)$$

where $\beta = 1/(k_{\rm B}T_{\rm cf})$, $\phi_{\sigma\sigma'}(r)$ is the pair potential, $h_{\sigma\sigma'}(r) = g_{\sigma\sigma'}(r) - 1$ is the pair correlation function, $c_{\sigma\sigma'}(r)$ is the direct correlation function, and $B_{\sigma\sigma'}(r)$ is the bridge function. Since the last function is neglected in the hypernetted-chain approximation, the Pauli potential $P_{\sigma\sigma'} = \delta_{\sigma\sigma'}P$ is determined from the pair correlation function in the ideal Fermi gas $h^0_{\sigma\sigma'} = \delta_{\sigma\sigma'}h^0_{\sigma\sigma}$ as

$$\beta\,P(r) = -\ln(h^0_{\sigma\sigma}(r)+1) + h^0_{\sigma\sigma}(r) - c^0_{\sigma\sigma}(r), \quad (10)$$

where the direct correlation function $c^0_{\sigma\sigma}(r)$ is given by the Ornstein–Zernike relation which is reduced to

$$h^0_{\sigma\sigma}(r) = c^0_{\sigma\sigma}(r) + n_\sigma \int {\rm d}\mathbf{r}' h^0_{\sigma\sigma}(|\mathbf{r}-\mathbf{r}'|)c^0_{\sigma\sigma}(r'). \quad (11)$$

In the case of $T = 0$ considered in this paper, the correlation function in the ideal gas in two dimensions is given by

$$h^0_{\sigma\sigma}(r) = -\left(\frac{2J_1(k^\sigma_{\rm F}r)}{k^\sigma_{\rm F}r}\right)^2, \quad (12)$$

where $k^\sigma_{\rm F} = 2(\pi n_\sigma)^{1/2}$. Here $J_1(z)$ is the Bessel function of the first order.

2.3. Diffraction effect

The pair potential is assumed to be given by

$$\phi_{\sigma\sigma'}(r) = P\delta_{\sigma\sigma'} + V^{\rm Coul}(r). \quad (13)$$

Here the second term $V^{\rm Coul}(r)$ is the Coulomb potential between electrons which is modified in order to take the effect of diffraction into account as [9]

$$V^{\rm Coul}(r) = \frac{1}{r}[1-\exp(-k_{\rm th}r)]. \quad (14)$$

Here $k_{\rm th}$ is a wavenumber of the order of the inverse of the thermal de Broglie wavelength.

The value of $k_{\rm th}$ is determined by solving the Schrödinger equation for a pair of two-dimensional electrons interacting via the potential $1/r$ and calculating the electron density at $r = 0$ [2]. The solution is written as

$$\Psi(r,\theta) = R_{kl}(r)\frac{1}{\sqrt{2\pi}}{\rm e}^{{\rm i}l\theta}, \quad (15)$$

$$R_{kl}(r) = C_{kl}\rho^l{\rm e}^{-\rho/2}F\left(l+\frac{1}{2}+\frac{\rm i}{2k}, 2l+1;\,\rho\right), \quad (16)$$

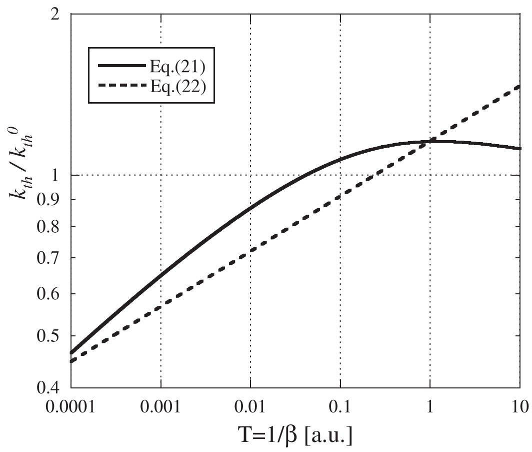

Figure 2. Values of $k_{\rm th}$ describing the effect of diffraction ($k^0_{\rm th}$ is the thermal de Broglie wavenumber). Solid and broken lines are for equations (21) and (22), respectively.

and

$$C_{kl} = \sqrt{k}2^{l+1/2}{\rm e}^{-\pi/(4k)}\frac{|\Gamma(l+\frac{1}{2}-\frac{\rm i}{2k})|}{\Gamma(2l+1)}, \quad (17)$$

where k is the momentum, $\rho = -2{\rm i}kr$, l is angular momentum and $F(\alpha,\gamma;z)$ is confluent hypergeometric function. The electron density at $r = 0$ and $l = 0$ is calculated as

$$|\Psi(r=0)|^2 = \frac{1}{2\pi}|R_{k0}(r=0)|^2 = k{\rm e}^{-\frac{\pi}{2k}}\frac{1}{\cosh(\frac{\pi}{2k})}. \quad (18)$$

Noting that the electron density of a free particle is given by

$$|\Phi(r=0)|^2 = \frac{1}{2\pi}(\sqrt{2\pi\,k})^2(J_{l=0}(kr=0))^2 = k, \quad (19)$$

we have the correlation function at $r = 0$ as

$$g(0) = \int_0^\infty k\frac{{\rm e}^{-\pi/(2k)}}{\cosh(\frac{\pi}{2k})}\,{\rm e}^{-\beta\epsilon}k\,{\rm d}k \bigg/ \int_0^\infty k\,{\rm e}^{-\beta\epsilon}k\,{\rm d}k, \quad (20)$$

where $\epsilon = k^2$. Regarding $g(0)$ as given by $\exp[-\beta\,V(r=0)]$, we obtain the relation

$$-\frac{\ln g(0)}{\beta{\rm e}^2k^0_{\rm th}} = \frac{k_{\rm th}}{k^0_{\rm th}}, \quad (21)$$

where $k^0_{\rm th} = (2\pi\,m^*\,T_{\rm cf})^{1/2}$ is the inverse of the thermal de Broglie wavelength with the reduced mass of the scattering electron pair $m^* = 1/2$. This ratio is plotted in figure 2. Perrot and Dharma-wardana have proposed the expression

$$k_{\rm th} = k^0_{\rm th} \times 1.158(T_{\rm cf})^{0.103} \quad (22)$$

for a two-dimensional system [2]. We observe that the proposed expression equation (22) for $k_{\rm th}/k^0_{\rm th}$ might be too simple and we may expect an improvement of the CHNC results by directly using equation (21). We show that this is the case in section 4.

2.4. Helmholtz free energy

The total Helmholtz free energy of the system is divided into the ideal gas part $F_{\rm id}$ and the exchange–correlation part $F_{\rm xc}$ as

$$F = F_{\rm id} + F_{\rm xc}. \tag{23}$$

At $T = 0$ the ideal gas part is given by

$$F_{\rm id} = \sum_{\sigma} F_{\rm id}^{\sigma} = n \sum_{\sigma=\pm 1} \frac{1}{4r_{\rm s}^2}(1+\sigma\zeta)^2. \tag{24}$$

The expectation value of the interaction part of the Hamiltonian, $\varepsilon_{\rm int}$, is given by the pair correlation functions as

$$\varepsilon_{\rm int} = \frac{n}{2}\int {\rm d}\mathbf{r}\frac{{\rm e}^2}{r}[\bar{g}(r) - 1], \tag{25}$$

where

$$\bar{g}(r) = \sum_{\sigma,\tau} \frac{n_\sigma}{n}\frac{n_\tau}{n} g_{\sigma\tau}(r). \tag{26}$$

The exchange–correlation part is obtained by an integration with respect to the scaled Coulomb coupling as

$$F_{\rm xc}(r_{\rm s},\zeta) = n\int_0^1 \frac{{\rm d}\lambda}{\lambda}\varepsilon_{\rm int}(\lambda e^2,\zeta). \tag{27}$$

Here $\varepsilon_{\rm int}(\lambda e^2, \zeta)$ is the expectation value of the interaction part of the Hamiltonian for the Coulomb coupling λe^2. At $T = 0$ the correlation energy per electron $E_{\rm c}$ is calculated from $E_{\rm c} = F_{\rm xc} - E_{\rm x}$, where $E_{\rm x}$ is the exchange part,

$$E_{\rm x}(r_{\rm s},\zeta) = -\frac{2^{3/2}}{3\pi\, r_{\rm s}}[(1+\zeta)^{3/2} + (1-\zeta)^{3/2}]. \tag{28}$$

3. Numerical simulation

The true Hamiltonian of our system with N electrons is given by

$$\hat{H} = -\sum_i^N \frac{\nabla_i^2}{2m} + \sum_{i>j}^N \frac{1}{r_{ij}}, \tag{29}$$

where $\mathbf{r}_i$ is the position of the particle i and $\mathbf{r}_{ij} = \mathbf{r}_i - \mathbf{r}_j$. After mapping, we perform numerical simulations of the classical system described by the Hamiltonian

$$\mathcal{H} = \sum_i^N \frac{\mathbf{p}_i^2}{2m} + \sum_{i>j}^N \frac{1-\exp(-k_{\rm th} r_{ij})}{r_{ij}} + \sum_{i>j}^N \delta_{\sigma_i\sigma_j} P(r_{ij}), \tag{30}$$

where σ_i is the spin of the particle i. The first term is the kinetic energy, the second term is the Coulomb interactions with the effect of diffraction, and the last term describes the Pauli potential between electrons with parallel spins.

In the case of two dimensions, it is shown that the asymptotic value of the Pauli potential for $r \to \infty$ is given by [2]

$$\beta P(k_{\rm F}^\sigma r) \sim \frac{\pi}{k_{\rm F}^\sigma r}. \tag{31}$$

Table 1. The size dependence of the Coulomb energy $\varepsilon_{\rm int}$ per electron in atomic units for systems of $N = 256$ and 512. As $T_{\rm q}$, the function Tq II is used.

	$N = 256$	$N = 512$
$r_{\rm s} = 40, \zeta = 0$	−0.025 739	−0.025 739
$r_{\rm s} = 40, \zeta = 1$	−0.025 502	−0.025 509
$r_{\rm s} = 20, \zeta = 0$	−0.049 929	−0.049 941
$r_{\rm s} = 20, \zeta = 1$	−0.049 741	−0.049 735

In our simulations, we apply an interpolation formula for the Pauli potential:

$$\beta\, P(k_{\rm F}^\sigma r) = \frac{\pi}{k_{\rm F}^\sigma r}[1 - \exp\{-1.95(k_{\rm F}^\sigma r)^{0.85}\}\cos(1.5 k_{\rm F}^\sigma r)]. \tag{32}$$

This satisfies the asymptotic behavior equation (31) and reproduces the values of Pauli potentials with a relative error less than 1% except for the region around $k_{\rm F}^\sigma r = 2$, $1.5 < k_{\rm F}^\sigma r < 2.5$, where the error is about 5%. We have confirmed that these errors do not influence our results given in section 4 by changing the fitting parameters. It has also been confirmed that the correlation function of the ideal gas, equation (12), is reproduced by numerical simulation using this interpolated Pauli potential with sufficient accuracy.

Monte Carlo and molecular dynamics simulations have been performed imposing the periodic boundary conditions. The Ewald method has been used to evaluate the forces caused by the Coulomb and the asymptotic part of the Pauli potential. For each combination of the parameters $r_{\rm s}$ and ζ, the system is relaxed to thermal equilibrium by the molecular dynamics and then the Monte Carlo method based on the Metropolis algorithm is applied. The numerical data have been obtained from the last part (more than 10^6 steps) of the long enough Monte Carlo steps which allow exact control of the temperature. Examples of the size dependence in the calculation of Coulomb energy per electron in the system are shown in table 1. On the basis of these results, we have adopted $N = 256$.

The values of $\varepsilon_{\rm int}$ are thus determined by simulations and integrated with respect to $r_{\rm s}$ from $r_{\rm s} = 0.5$ to the target value of $r_{\rm s}$ in order to obtain $F_{\rm xc}(r_{\rm s},\zeta)$ and the Helmholtz free energy. The relative error of the resultant free energy is less than 0.1% for all regions of $r_{\rm s}$ values. These errors are sufficiently small for deriving the results shown in section 4.

4. Results and discussion

We first compare the results for the correlation energy obtained by our method of simulations adopting Tq I and Tq II with the DMC results [7, 8], in figure 3. Here equation (22) is used for the diffraction effect. We find that Tq II gives much better agreement with DMC values especially in the domain $r_{\rm s} \leqslant 10$. Since our simulation automatically takes the contribution of the bridge function into account and Tq I and Tq II are determined respectively with and without the contribution of the bridge function [2, 4], this result seems somewhat puzzling. Considering, however, that the accuracy in the reproduction of DMC results by Tq II is not easy to extract from published

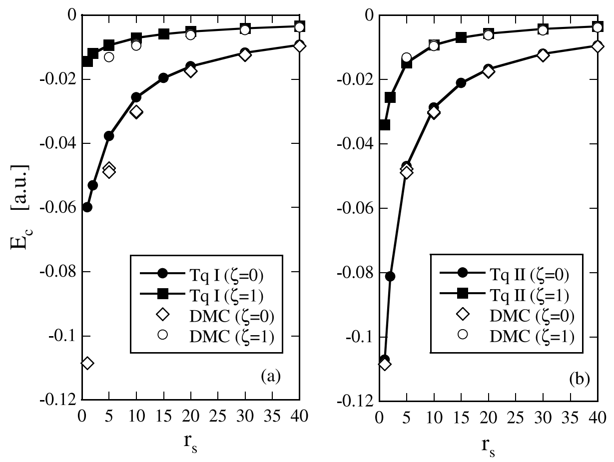

Figure 3. Correlation energy E_c in atomic units obtained by classical-map simulations in comparison with DMC results [7, 8]. The quantum temperature Tq I (a) or Tq II (b). The effect of diffraction is described by equation (22) in both cases.

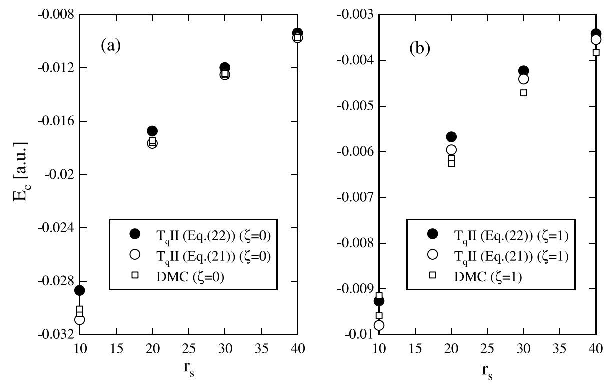

Figure 5. Correlation energy E_c in atomic units obtained by classical-map simulations using Tq II with equations (22) and (21) compared with DMC results [7, 8] for (a) $\zeta = 0$ and (b) $\zeta = 1$.

data and our purpose is to obtain a better expression for the quantum temperature, we do not make further investigations of the reason here.

As for the effect of diffraction, the pair distribution function for an unpolarized system at $r_s = 20$ with Tq II and the effect of diffraction expressed by equation (22) and equation (21) are compared with the DMC results in figure 4. We find that the first peaks and the first valley of the pair distribution function are lower and shallower, respectively, than those for DMC results. The results of CHNC analyses using integral equations, figure 2 of [2] and figure 3 of [4], also give similar results and the results of our simulations are consistent with those of integral equation analyses. When the effect of diffraction is taken into account by equation (21), however, about half of the deviation from the DMC results at the first peak is recovered. Though the improvement in the depth at the first valley is still small, it is clear that equation (21) gives a better description of the effect of diffraction.

We summarize the values of the correlation energy for $\zeta = 0$ and $\zeta = 1$ in tables 2 and 3, respectively. They include the values obtained with (Tq II and equation (22)), (Tq II and equation (21)), and reported DMC values. They are plotted in figure 5 and we observe a significant improvement in reproduction of the DMC results especially in the case of $\zeta = 0$. When $\zeta = 0$, the effect of diffraction plays a more important role near $r = 0$ as compared with the case for $\zeta = 1$, where the repulsive Pauli potential working for all pairs reduces the effect of diffraction.

Values of the Helmholtz free energy in atomic units obtained by our simulations for $\zeta = 0$ and $\zeta = 1$ are summarized in tables 4 and 5, respectively, giving the values obtained with (Tq I and equation (22)), (Tq II and equation (22)), (Tq II and equation (21)), and reported DMC values. We confirm that values obtained with (Tq II and equation (21)) give significantly better agreement with DMC values.

In order to discuss the ground state polarization, we plot the excess Helmholtz free energy of the $\zeta = 1$ state over the $\zeta = 0$ state obtained with the combination

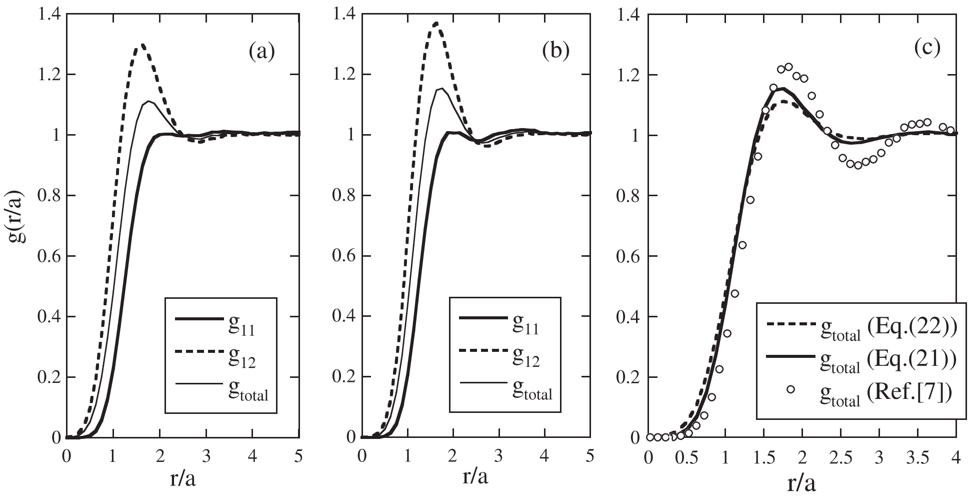

Figure 4. Pair distribution functions obtained by classical-map simulations for $r_s = 20$ and $\zeta = 0$. The quantum temperature Tq II is adopted and the diffraction effect is described either (a) by equation (22) or (b) by equation (21). In (c), total electron distributions obtained with equation (21) (solid line) and with equation (22) (broken line) are compared with DMC results [7].

Table 2. Correlation energy E_c ($\zeta = 0$) in atomic units versus r_s. Results obtained with Tq I + equation (22), Tq II + equation (22) and Tq II + equation (21) are compared with DMC values.

r_s	E_c (Tq I + (22))	E_c (Tq II + (22))	E_c (Tq II + (21))	E_c (Reference [7])	E_c (Reference [8])
1	−0.059 92	−0.107 09	−0.118 93	−0.108 5	
2	−0.053 15	−0.081 20	−0.089 45		
5	−0.037 75	−0.046 91	−0.051 33	−0.047 75	−0.048 91
10	−0.025 67	−0.028 70	−0.030 89	−0.030 43	−0.030 09
20	−0.016 01	−0.016 74	−0.017 66	−0.017 58	−0.017 44
30	−0.011 74	−0.011 98	−0.012 52	−0.012 51	−0.012 43
40	−0.009 30	−0.009 39	−0.009 74		−0.009 70

Table 3. The same as table 2 but for the case of $\zeta = 1$.

r_s	E_c (Tq I + (22))	E_c (Tq II + (22))	E_c (Tq II + (21))	E_c (Reference [7])	E_c (Reference [8])
1	−0.014 45	−0.034 09	−0.036 23		
2	−0.011 98	−0.025 45	−0.026 56		
5	−0.009 41	−0.014 78	−0.015 60	−0.013 16	−0.013 56
10	−0.007 11	−0.009 27	−0.009 80	−0.009 15	−0.009 59
20	−0.005 17	−0.005 68	−0.005 96	−0.006 15	−0.006 26
30	−0.004 13	−0.004 23	−0.004 41	−0.004 71	−0.004 73
40	−0.003 46	−0.003 42	−0.003 55	−0.003 83	−0.003 83

Table 4. Helmholtz free energy ($\zeta = 0$) in atomic units versus r_s. Results obtained with Tq I + equation (22), Tq II + equation (22) and Tq II + equation (21) are compared with DMC values.

r_s	F (Tq I + (22))	F (Tq II + (22))	F (Tq II + (21))	F (Reference [7])	F (Reference [8])	F (Reference [10])
1	−0.160 15	−0.207 32	−0.219 16			
2	−0.228 27	−0.256 32	−0.264 56			
5	−0.137 80	−0.146 96	−0.151 37	−0.149 8	−0.149 0	−0.149 52
10	−0.080 695	−0.083 718	−0.085 917	−0.085 45	−0.085 12	−0.085 43
15	−0.057 452	−0.058 844	−0.060 184			
20	−0.044 770	−0.045 502	−0.046 425	−0.046 34	−0.046 20	−0.046 28
30	−0.031 189	−0.031 434	−0.031 968	−0.031 96	−0.031 87	−0.031 94
40	−0.023 993	−0.024 082	−0.024 437		−0.024 39	

Table 5. The same as table 4 but for the case of $\zeta = 1$.

r_s	F (Tq I + (22))	F (Tq II + (22))	F (Tq II + (21))	F (Reference [7])	F (Reference [8])	F (Reference [10])
1	0.136 67	0.117 03	0.114 89			
2	−0.186 42	−0.199 89	−0.201 00			
5	−0.139 18	−0.144 55	−0.145 37	−0.142 9	−0.143 3	−0.143 61
10	−0.081 994	−0.084 155	−0.084 690	−0.084 04	−0.084 48	−0.084 58
15	−0.058 074	−0.059 117	−0.059 493			
20	−0.045 117	−0.045 621	−0.045 902	−0.046 12	−0.046 20	−0.046 25
30	−0.031 318	−0.031 417	−0.031 595	−0.031 90	−0.031 92	−0.031 94
40	−0.024 052	−0.024 016	−0.024 145	−0.024 42	−0.024 42	

(Tq II and equation (21)) in figure 6. We observe that the ground state is always unpolarized in the domain $r_s < 40$. The difference in free energy, however, is very small for $20 < r_s$ and we are unable to make any clear statement on the polarization in this domain. These results are consistent with the previous works using DMC methods for two-dimensional electron fluid [4, 7, 10] which are not conclusive on the polarization at large r_s before Wigner lattice formation. Though CHNC analysis using integral equations predicts increase of the polarized domain at low temperatures with increase of the temperature [3], the result for $T = 0$ does not seem to be more conclusive than quantum simulations.

5. Conclusion

In this paper, we have proposed a method for simulating quantum systems on the basis of the CHNC mapping. We have given important information on the selection of the quantum temperature with an improved treatment of the effect of the diffraction which leads to significantly improved reproduction of the known results of quantum simulations.

Since our classical simulation is a method designed to reproduce the results of quantum simulations, it cannot answer any questions which are not settled by quantum simulations. Our method of simulation, however, is much easier to perform than first-principle quantum simulations and

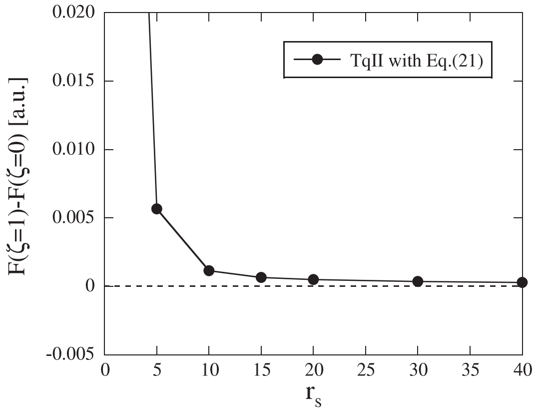

Figure 6. Difference of the Helmholtz free energies $F(r_s, \zeta = 1)$ and $F(r_s, \zeta = 0)$ in atomic units obtained via classical-map simulations using Tq II and equation (21).

we have many cases where quantum simulations are difficult and our classical-map simulation can give clear answers. These cases include systems that are finite but not so small sized, and those with complex geometry. For example, we have analyzed electrons confined in quantum dots by this method and shown the possibility of spin polarization [11]. The results given here may serve as a part of a basis for further application of this classical-map simulation.

References

[1] Dharma-wardana M W C and Perrot F 2000 *Phys. Rev. Lett.* **84** 959

[2] Perrot F and Dharma-wardana M W C 2001 *Phys. Rev. Lett.* **87** 206404

[3] Dharma-wardana M W C and Perrot F 2003 *Phys. Rev. Lett.* **90** 136601

[4] Bulutay C and Tanatar B 2002 *Phys. Rev.* B **65** 195116

[5] Khanh N Q and Totsuji H 2003 *Solid State Commun.* **129** 37

[6] Khanh N Q and Totsuji H 2004 *Phys. Rev.* B **69** 165110

[7] Tanatar B and Ceperley D M 1989 *Phys. Rev.* B **39** 5005

[8] Rapisarda F and Senatore G 1996 *Aust. J. Phys.* **49** 161

[9] Minoo H, Gombert M M and Deutsch C 1981 *Phys. Rev.* A **23** 924

[10] Attaccalite C, Moroni S, Gori-Giorgi P and Bachelet G B 2002 *Phys. Rev. Lett.* **88** 256601

[11] Miyake T, Totsuji C, Nakanishi K, Tsuruta K and Totsuji H 2008 *Phys. Lett.* A **372** 6197